

# Ab Initio Calculation of Homogeneous Outer Sphere Electron Transfer Rates: Application to $M(\text{OH}_2)_6^{3+/2+}$ Redox Couples

Kevin M. Rosso\* and James R. Rustad

W. R. Wiley Environmental Molecular Sciences Laboratory, Pacific Northwest National Laboratory,  
P.O. Box 999, MSIN K8-96 Richland, Washington 99352

Received: November 23, 1999; In Final Form: March 29, 2000

Ab initio density functional theory calculations are applied to the prediction of homogeneous outer sphere electron transfer rates within the classical Marcus formalism for a series of transition metal hexaquo ions in a background electrolyte. Reorganization energies, frequency factors, electronic transmission coefficients, and the effective electron transfer distances are calculated. Theoretical inner sphere contributions to the reorganization energies correlate very well with total reorganization energies estimated from experimental self-exchange rates. Important energy contributions arising from Jahn–Teller distortions are accurately included in the inner sphere term. Effective electron transfer distances are found to be only slightly longer than the sum of the average calculated M–O distances. Calculated adiabatic self-exchange rates agree well with observed self-exchange rates. The driving force for bimolecular electron transfers, calculated from total energy differences, is found to compare well with estimations using experimental reduction potentials to within 4 kJ/mol. The choice of basis set is found to be very important in these calculations, and for this system, the 6-311+G basis set outperforms DZVP. The methods presented provide a convenient means to produce usefully accurate parameters for Marcus theory to predict outer sphere electron transfer rates.

## 1. Introduction

Knowing the rates of individual electron transfer reactions can be fundamentally important in understanding the behavior of overall redox processes in natural waters. This is because any particular electron transfer step in a reaction series can be slow, thereby controlling the overall rate. Rate limiting electron transfer can play a dominant role in trace metal cycling and the speciation and transport of contaminants in the environment. Examples include the slow oxidation of  $\text{Mn(II)}$ <sup>1</sup> and  $\text{H}_2\text{S}$ <sup>2,3</sup> by  $\text{O}_2$  and the persistence of intermediate organic degradation products in oxic groundwaters.<sup>4–7</sup> Predictive models based on thermodynamic redox equilibria are inadequate in such cases and must incorporate disequilibrium kinetics.<sup>8,9</sup> Knowing the rates of the component elementary electron transfer steps is a necessary prerequisite to developing accurate overall models.

Electron transfer reactions can generally be subdivided into two types: those following an inner sphere mechanism vs those following an outer sphere mechanism. In any particular overall reaction, both pathways can operate in parallel. However, the preference of inner vs outer sphere can change with solution conditions such as pH because it can affect the lability of inner shell ligands (e.g., 10). The ability to predict electron transfer rates for a particular pathway as a function of reactant speciation would be invaluable for the interpretation of macroscopic kinetic experiments.

Marcus<sup>11</sup> developed a useful quantitative theory for predicting outer sphere homogeneous electron transfer rates in solution, and later extended the theory to heterogeneous electron transfer at interfaces (ref 12 and references therein). The theory also has been demonstrated to be useful in understanding electron transfer in biomolecules,<sup>13</sup> intrasurface charge transfer,<sup>14</sup> and scanning tunneling microscopy (STM) data.<sup>15,16</sup> The basic

principle relates the activation free energy ( $\Delta G^*$ ) for the electron transfer step to the driving force ( $\Delta G^\circ$ ) and the reorganization energy ( $\lambda$ ). The latter is usually taken as the sum of the energies required to reorganize the molecular structure of the reactants ( $\lambda_{\text{is}}$  = inner sphere contribution) and the surrounding solvent molecules ( $\lambda_{\text{os}}$  = outer sphere contribution) to the configuration compatible with electron transfer. Total reorganization energies are measurable quantities under certain circumstances using electron spin resonance line-broadening experiments or STM.<sup>16</sup> These experimental approaches are restricted to ideal conditions with stable molecules and can be tedious to implement. At the same time, measurement of the inner and outer sphere contributions to the reorganization energy in the chemical conditions of interest is quite rare. Since the usefulness of Marcus theory hinges on obtaining accurate estimations of the reorganization energy, it is natural to consider the utility of modern molecular modeling techniques for this purpose.

A variety of molecular modeling approaches have been applied to calculating either  $\lambda_{\text{is}}$  or  $\lambda_{\text{os}}$  for homogeneous and heterogeneous electron transfer.<sup>17–20</sup> Rigorous calculations of  $\lambda_{\text{os}}$  require dynamic simulation of fluctuating solvent molecules,<sup>21,22</sup> but this approach seems far from practical. The original dielectric continuum treatment by Marcus is in widespread use and can be sufficiently accurate, with knowledge of the effective radii of the reactants. Theoretical approaches to estimate  $\lambda_{\text{is}}$  are surprisingly few, and the “best” approach is still a matter of debate. However, several commonalities are clear. Ab initio cluster calculations arrive at more accurate potential energy surfaces for the reactant molecules than parametrized electrostatic approaches.<sup>23–25</sup> Hartree–Fock methods overestimate  $\lambda_{\text{is}}$  and the effects of electron correlation must be taken into account.<sup>26,27</sup> Most of these previous approaches arrive at  $\lambda_{\text{is}}$  using force constants from a cumbersome procedure of fitting polynomial expressions to the ab initio based potential

\* Corresponding author. E-mail: kevin.rosso@pnl.gov.

energy surfaces. Using Moller–Plesset second-order perturbation theory (MP2) for the geometry optimizations of organic  $\pi$ -systems, Klimkans and Larsson<sup>26</sup> suggested that  $\lambda_{\text{is}}$  could be calculated in a convenient way from the total energies of the isolated reactant molecules in their ground and excited electronic states. However, to our knowledge, a benchmarking of this approach against experimental data has not been performed.

The purpose of this investigation is to evaluate density functional theory (DFT) ab initio cluster calculations as a means to derive, in a simple but sufficiently accurate way, the Marcus parameters for homogeneous outer sphere electron transfer. We chose a series of  $M(\text{OH}_2)_6^{3+/2+}$  using  $M = \text{V}, \text{Cr}, \text{Mn}, \text{Fe},$  and  $\text{Co}$  as the case study for several reasons. These five first row transition metal aquo ions are expected to follow an outer sphere pathway for self-exchange.<sup>28,29</sup> This allows the total reorganization energy to be estimated from experimental self-exchange rates through the Marcus relations. Experimental self-exchange rates for these complexes are well-known and vary widely, spanning 5 orders of magnitude. Also, because they also undergo electron self-exchange without the tendency to hydrolyze or change coordination numbers, differences in the self-exchange rates are due mostly to differences in  $\lambda_{\text{is}}$ . Although the trivalent ions typically exist only in trace quantities in natural aquatic environments, self- and bimolecular exchange kinetics between these trace ions are nonetheless of geochemical importance in the redox cycling of metals and atmospheric chemistry.<sup>30</sup>

## 2. Outer Sphere Electron Transfer Theory

Complete descriptions of the theory are available in the literature.<sup>13,31–33</sup> The following is a brief summary of the equations which were used to calculate outer-sphere electron transfer rates for the self-exchange or homogeneous bimolecular redox reactions in this study. Observable rates of self-exchange or homogeneous redox exchange involve the following basic steps: (I) diffusion of the reactants together to form the precursor complex, (II) electron transfer within the complex to form the successor complex, and (III) dissociation of the successor complex. These can be written in the context of self-exchange reactions as



Using the steady state approximation and assuming the reaction is not diffusion limited and that dissociation in step III is fast, the net rate that is usually observed in experiment is due only to the equilibrium constant for the formation of the precursor complex ( $K_{\text{pre}}$ ) and the rate of electron transfer ( $k_{\text{et}}$ ):

$$k_{\text{obs}} = K_{\text{pre}} k_{\text{et}} \quad (1)$$

$K_{\text{pre}}$  is described as

$$K_{\text{pre}} = 4\pi N R^2 dR \exp(-w/RT) \quad (2)$$

where  $N$  is Avogadro's number,  $R$  is the effective separation of the reactants at their closest approach,  $dR$  is the effective reaction zone thickness, and  $w$  is the Coulombic work to bring the reactants together.<sup>34</sup> A commonly used value for  $dR$ , also used here, is  $1/1.2$ .<sup>31,32</sup> The electrostatic energy term  $w$  depends on

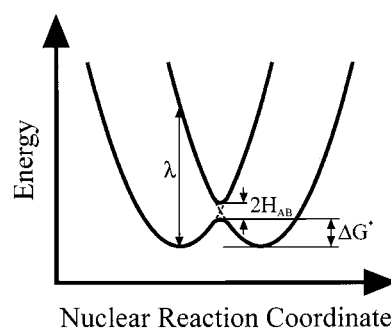


**Figure 1.** Potential energy of the reactants (left parabola) and products (right parabola) as a function of the nuclear configuration for a self-exchange reaction where there is no net free energy change. For the redox couples in this study, splitting in the intersection region, exaggerated in the diagram, is small due to weak electronic coupling of the reactants.  $H_{\text{AB}}$  is approximately 2 orders of magnitude smaller than  $\lambda$ , leading to slow electron transfer. The activation energy barrier ( $\Delta G^*$ ) is then approximately equal to  $\lambda/4$ .

the charges of the reactants, the separation of the reactants  $R$ , and the dielectric properties of the solvent corrected for ionic strength. Various equations have been derived in this regard. Most are based in Debye–Hückel theory and are therefore approximate but sufficiently accurate below ionic strengths about 2–3 M. For simplicity, the expression employed in a study by Weaver and Lee<sup>35</sup> was used in this study:

$$w = (1/4\pi\epsilon_0) Z_1 Z_2 e^2 N / \epsilon_s R_m (1 + BR_{\text{A}} \mu^{1/2}) \quad (3)$$

where the factor  $1/4\pi\epsilon_0$  equals  $8.988 \times 10^9 \text{ N}\cdot\text{m}^2/\text{C}^2$ ,  $Z_1$  and  $Z_2$  are the charges on the reactants (+2 and +3 throughout this study),  $e$  is the electron charge ( $1.602 \times 10^{-19} \text{ C}$ ),  $\epsilon_s$  is the static dielectric constant of the solvent (78.39 for  $\text{H}_2\text{O}$  at 25 °C),  $R_m$  is  $R$  expressed in meters,  $B$  is a Debye–Hückel parameter, and  $\mu$  is the ionic strength. The factor  $BR_{\text{A}}$  is a unitless parameter on the order of unity in practice.<sup>36</sup> The value of  $B$  at 25 °C is 0.328 for  $R$  expressed in angstroms ( $R_{\text{A}}$ ).<sup>37</sup> Using these values,  $w$  comes out in joules per mole.

Within the activated complex, the rate of electron transfer ( $k_{\text{et}}$ , eq 1) is based on the rate of fluctuation of the electronic state of the precursor complex in the direction of the electronic state of the successor complex due to thermally induced changes in the nuclear configuration. The two states can be diagrammed as parabolic total energy surfaces as a function of a nuclear configuration coordinate as shown in Figure 1. Electron transfer takes place in the intersection region of the two curves representing the point when the precursor complex has been activated to the configuration of the transition state. Here, the probability of electron transfer is subdivided into two classes: adiabatic and nonadiabatic. The former implies a high degree of mixing of reactant orbitals, causing the intersection region to be split and smoothed (Figure 1) to the degree that the probability of electron transfer is effectively 100% once the transition state configuration is reached. The latter describes reactions where the orbital mixing is so small that little splitting occurs and the probability of electron transfer is much lower, often arising from structural or steric hindrances causing a large separation between the redox active centers. The rate of both types of electron transfer can be written as

$$k_{\text{et}} = \nu \Gamma \kappa \exp(-\Delta G^*/RT) \quad (4)$$

where  $\nu$  is the nuclear frequency factor ( $\text{s}^{-1}$ ),  $\Gamma$  is a nuclear tunneling factor,  $\kappa$  is the electronic transmission coefficient, and

$\Delta G^*$  is the free energy of activation. At room temperature, nuclear tunneling does not typically contribute significantly to the electron transfer rate, so  $\Gamma$  is assumed equal to unity<sup>13</sup> and is such throughout this study. In contrast, the electronic coupling between the redox pairs in this study is expected to be weak,<sup>38,39</sup> and therefore  $\kappa$  is much lower than unity and must be treated explicitly (see next section). In doing so, we assume an electron transfer probability that is significantly less than 100% once the transition state is reached (nonadiabatic).

Marcus developed a simple but useful statistical mechanical model relating the free energy of activation ( $\Delta G^*$ ) to the driving force of the electron transfer step ( $\Delta G^\circ$ ) and the reorganization energy ( $\lambda$ ):

$$\Delta G^* = (\Delta G^\circ + \lambda)^2/4\lambda \quad (5)$$

For self-exchange reactions,  $\Delta G^\circ = 0$  and thus  $\Delta G^*$  equates simply to  $\lambda/4$  and is referred to as the intrinsic electron exchange barrier (Figure 1). In bimolecular redox reactions  $\Delta G^\circ \neq 0$  and  $\lambda$  can be obtained from the Marcus cross relation:

$$\lambda = (\lambda_1 + \lambda_2)/2 \quad (6)$$

where  $\lambda_1$  and  $\lambda_2$  are the self-exchange reorganization energies for reactants 1 and 2, respectively. Where formal reduction potentials are available,  $\Delta G^\circ$  can be obtained from

$$\Delta G^\circ = -nF(E_{\text{red}} - E_{\text{ox}}) \quad (7)$$

where  $n$  is the number of moles of electrons transferred,  $F$  is the Faraday constant, and  $E_{\text{red}}$  and  $E_{\text{ox}}$  are the standard reduction potentials for the respective half-reactions. Since the Marcus relations are only applicable to one-electron-transfer reactions,  $n$  in eq 7 will be equal to 1 throughout this study. It should also be noted that  $\Delta G^\circ$  should be corrected for the difference in electrostatic work required to bring the reactants together and that for the products.<sup>32</sup> In this study, because the charges of the reactants equals the charges of the products and the changes in the effective radii of the reactants and products are small, this correction is insignificant.

The reorganization energy  $\lambda$  is the energy required to move all the precursor complex atoms, including the solvent molecules, from their equilibrium positions to the equilibrium positions of the successor complex without transferring the electron (Figure 1). Contributions to  $\lambda$  are separated into that from the inner sphere atoms ( $\lambda_{\text{is}}$ ), in this case the  $\text{M}(\text{OH}_2)_6$  cluster, and the outer sphere solvent atoms ( $\lambda_{\text{os}}$ ), in this case the second hydration sphere, with  $\lambda = \lambda_{\text{is}} + \lambda_{\text{os}}$ .  $\lambda_{\text{os}}$  is due to the work of reorganizing solvent molecules surrounding the activated complex and has been successfully treated from continuum theory<sup>11</sup> using

$$\lambda_{\text{os}} = (\Delta q)^2 (1/2r_1 + 1/2r_2 - 1/R)(1/D_{\text{op}} - 1/\epsilon_s) \quad (8)$$

where  $q$  is the charge transferred,  $r_1$  and  $r_2$  are the effective radii of the reactant molecules with  $r_1 + r_2 = R$ , and  $D_{\text{op}}$  is the optical dielectric constant of the solvent (equals the index of refraction squared). Using angstroms,  $\lambda_{\text{os}}$  comes out in electronvolts.

### 3. Theoretical Methods

**Inner Sphere Reorganization Energies ( $\lambda_{\text{is}}$ ).** The Klimkans and Larsson study of organic  $\pi$ -systems suggested that  $\lambda_{\text{is}}$  for self-exchange reactions could be calculated from the ab initio

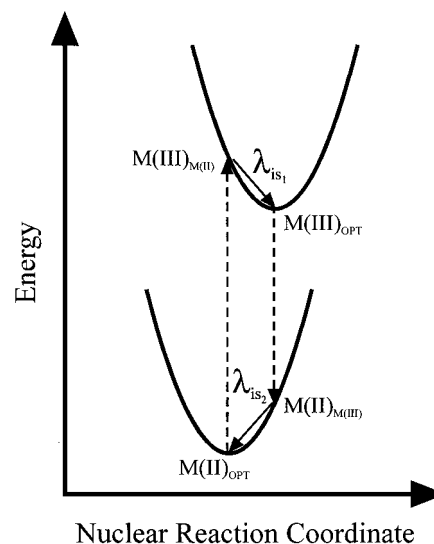


**Figure 2.** Schematic illustration of the approach for the calculation of inner sphere reorganization energies (modified from Klimkans and Larsson). Potential energy curves are shifted vertically reflecting the total energy differences between a  $\text{M}(\text{III})(\text{OH}_2)_6$  complex ( $n$  electrons) and a  $\text{M}(\text{II})(\text{OH}_2)_6$  complex ( $n + 1$  electrons). The  $\text{M}(\text{II})_{\text{OPT}} - \text{M}(\text{III})_{\text{M(II)}}$  energy difference is equivalent to the vertical ionization potential of  $\text{M}(\text{II})_{\text{OPT}}$ . The  $\text{M}(\text{III})_{\text{OPT}} - \text{M}(\text{II})_{\text{M(III)}}$  energy difference is the vertical electron affinity of  $\text{M}(\text{III})_{\text{OPT}}$ . The inner sphere reorganization energy =  $\lambda_{\text{is}_1} + \lambda_{\text{is}_2}$ .

total energy differences of four gas-phase clusters. Using the self-exchange example given in reaction II above, this procedure breaks  $\lambda_{\text{is}}$  into two components:

$$\lambda_{\text{is}_1} = E(\text{M}(\text{III})_{\text{M(II)}}) - E(\text{M}(\text{III})_{\text{OPT}}) \quad (9)$$

$$\lambda_{\text{is}_2} = E(\text{M}(\text{II})_{\text{M(III)}}) - E(\text{M}(\text{II})_{\text{OPT}}) \quad (10)$$

with

$$\lambda_{\text{is}} = \lambda_{\text{is}_1} + \lambda_{\text{is}_2} \quad (11)$$

where  $E$  indicates the total electronic energy and the subscript is a reference to the configuration of the cluster with "OPT" indicating the calculated minimum energy structure.  $\text{M}(\text{III})_{\text{M(II)}}$  then represents a single point energy calculation of  $\text{M}(\text{III})$  frozen in the optimized  $\text{M}(\text{II})$  configuration, and vice versa for  $\text{M}(\text{II})_{\text{M(III)}}$ . The overall procedure is diagrammed in Figure 2. We adopt this approach in this study for its simplicity. It has not been applied to transition metal complexes elsewhere in the literature to our knowledge.

**Frequency Factor ( $\nu$ ).** The frequency factor  $\nu$  can be taken as the sum of the weighted contributions of all the normal mode force constants to  $\lambda$ .<sup>13</sup> Presumably, the inner sphere reorganization energy for the  $\text{M}(\text{OH}_2)_6$  clusters is largely due to  $\text{M}-\text{O}$  bond stretching, hence we used the calculated symmetric stretching frequencies for the self-exchange reactants in

$$\nu = [(c\nu_{\text{M(II)}})^2 + (c\nu_{\text{M(III)}})^2]/2^{0.5} \quad (12)$$

where  $c$  (m/s) is the speed of light, and  $\nu_{\text{M(II)}}$  and  $\nu_{\text{M(III)}}$  are the calculated symmetric stretching frequencies ( $\text{m}^{-1}$ ) for  $\text{M}(\text{II})(\text{OH}_2)_6$  and  $\text{M}(\text{III})(\text{OH}_2)_6$ , respectively. This assumes an equal contribution of  $\nu_{\text{M(II)}}$  and  $\nu_{\text{M(III)}}$  to  $\lambda_{\text{is}}$  which is justified in this study because, in the self-exchange reactions, most calculated values of  $\lambda_{\text{is}_1}$  and  $\lambda_{\text{is}_2}$  turn out to be nearly equal. For bimolecular

reactions, we use the geometric mean of the self-exchange frequencies:<sup>32</sup>

$$\nu = (\nu_1\nu_2)^{0.5} \quad (13)$$

where  $\nu_1$  and  $\nu_2$  are the calculated frequency factors for the self-exchange reactions of the reactants.

**Electronic Transmission Coefficient ( $\kappa$ ).** Splitting of the potential energy surfaces in the intersection region due to electronic interaction of the reactants is treated quantitatively via the electronic coupling matrix element  $H_{AB}$  (see Figure 1).  $H_{AB}$  is dependent on the separation of the redox centers in the encounter complex and is highly sensitive to a particular structural conformation,<sup>39</sup> calling into question the practical usefulness of its rigorous determination from static calculations. Therefore, in this study, we adopt an internally consistent set of  $H_{AB}$  values derived quasi-experimentally for the redox couples in their dynamic state.<sup>25</sup> These are combined with the calculated values for  $\nu$  to estimate  $\kappa$  using<sup>29</sup>

$$\kappa = 2[1 - \exp(-\nu_{el}/2\nu)]/[2 - \exp(-\nu_{el}/2\nu)] \quad (14)$$

where  $\nu_{el}$  is the frequency of electron transfer ( $\text{s}^{-1}$ ) within the activated complex given by<sup>29</sup>

$$\nu_{el} = 2H_{AB}^2/h(\pi^3/\lambda RT) \quad (15)$$

where  $h$  is Planck's constant. For the biomolecular reactions,  $\kappa$  was calculated similarly to  $\nu$  in eq 13.

**Effective Electron Transfer Distance ( $R$ ).** The effective electron transfer distance  $R$  is traditionally a somewhat ambiguous parameter, although it is generally related to the size of the reactant species.<sup>40</sup> The ab initio methods used here can provide highly accurate geometries and bond lengths, including Jahn–Teller distortions for  $\text{Mn}(\text{III})(\text{OH}_2)_6$  and  $\text{Cr}(\text{II})(\text{OH}_2)_6$ , but the relationship between these subtle differences in bond lengths in individual reactants and the effective electron transfer distance  $R$  is unclear. We retain some of these differences in the  $M(\text{OH}_2)_6$  clusters by averaging the six calculated M–O bond lengths and using this value for the base radius of the cluster. The effective radius of the cluster,  $r$ , however, is commonly thought to be somewhat larger than the cluster itself by values up to 1.4 Å.<sup>40</sup> Similarly, we leave room for an adjustable distance parameter,  $x$ , that is common to all the clusters within the suite of calculations using

$$r = r_{M-O} + x \quad (16)$$

and

$$R = r_{1\text{ M-O}} + r_{2\text{ M-O}} + 2x \quad (17)$$

where  $r_{1\text{ M-O}}$  and  $r_{2\text{ M-O}}$  are the average calculated M–O bond lengths of the reactants. The value of  $x$  was determined for each suite of calculations as follows. Using the calculated value of  $R$  with  $x$  initially set to zero, observed self-exchange rates were corrected for  $K_{\text{pre}}$  and electrostatic work using their respective experimental ionic strengths and eq 3, giving an estimate of  $k_{\text{et}}$ . Using the calculated values of  $\nu$  and  $\kappa$  and eqs 4 and 5, we arrived at an estimate of  $\lambda$  from the experimental rate data. The ab initio total energy approach outlined in eqs 9–11 was used to calculate  $\lambda_{\text{is}}$ , eq 8 was used with  $R$  to calculate  $\lambda_{\text{os}}$ , and the sum was used as the theoretical estimate for  $\lambda$ . The theoretical value for  $\lambda$  and its best estimate from experiment were plotted against each other and linearly regressed. The  $x$  value was then adjusted so that the trend between the calculated and experi-

mental  $\lambda$ 's passed through zero, as it should in principle. We note that the choice to use calculated values of  $R$  and  $\nu$  to compute the “best” guess for the experimental  $\lambda$  was to avoid introducing additional error in the estimate of  $x$ .

**Ab Initio Methods.** We performed the ab initio calculations using Gaussian94<sup>41</sup> on Silicon Graphics R10k-based workstations. We chose to utilize the B3LYP hybrid DFT method<sup>42,43</sup> as it has been shown to be sufficiently accurate to provide useful results on a variety of molecules.<sup>44–47</sup> The calculations were repeated using two basis sets: a so-called “DFT orbital” DZVP set<sup>48</sup> and a Pople-type 6-311+G set were used. The latter consists of a Wachters–Hay 6-311G set<sup>49,50</sup> with an added diffuse function (“+”),<sup>51</sup> The DZVP set was chosen because of its demonstrated usefulness in the calculation of relative proton binding energies for the trivalent transition metal hexaquo ions considered in this study,<sup>47</sup> and the 6-311+G set was chosen because of the accurate total free energies obtained<sup>46</sup> for  $\text{Fe}(\text{III})(\text{OH}_2)_6$ . Starting  $M(\text{OH}_2)_6$  structures and initial guess wave function were obtained from geometry optimizations at the Hartree–Fock level of theory using a 3-21G basis set. All optimizations were performed without symmetry restrictions. As most of the trivalent first row transition metals are in a high spin state in aqueous solution, the cluster calculations were performed using a high spin restriction. In our series of  $M(\text{OH}_2)_6$  complexes, Co(III) is the only exception because it is expected to be predominantly in a low spin configuration with the  $t_{2g}$  nonbonding set filled with six electrons.<sup>52</sup> For simplicity and consistency within this  $M(\text{OH}_2)_6$  series, we chose to model the Co self-exchange process as a simple, one-electron, high spin exchange. Mulliken population analyses of the distribution of charges and spin density on the metal atom for the optimized and frozen geometry configurations were checked to be consistent with the desired charge and spin state. Frequency calculations, as implemented in Gaussian94, were performed on the final optimized clusters to ensure convergence to a true minimum, to calculate the symmetric stretching frequency, and to obtain estimates of the thermochemical contributions to the total energy (298.15 K, 1 atm standard state; zero point, thermal, enthalpic, and entropic corrections to the electronic energy).

#### 4. Results and Discussion

**Self-Exchange Reactions.** The series of five  $M(\text{OH}_2)_6$  clusters are not expected to have significant differences in solvent reorganization energies because the small differences in the average bond lengths for the reactant molecules equate to minor differences in  $\lambda_{\text{os}}$  ( $\sim 0.04$  eV). Likewise, values for  $\nu$  derived from calculated symmetric stretching frequencies are expected to be alike in magnitude ( $\sim 10^{13}$ ), and similarly,  $\kappa$  is expected to vary within an order of magnitude of the  $10^{-2}$  range.<sup>53</sup> In similar ionic strength solutions, the work terms should also be similar because all reactant charges are +2 and +3. Hence, we expect that most of the differences in observed rates are a reflection of differences in  $\lambda_{\text{is}}$ . Calculated values of  $\lambda_{\text{is}1}$ ,  $\lambda_{\text{is}2}$ , and  $\lambda_{\text{is}}$  for the transition metal hexaquo ion series from our ab initio calculations performed using both the DZVP and 6-311+G basis sets are reported in Table 1. Total electronic energies for the optimized  $M(\text{OH}_2)_6$  clusters and the  $M(\text{OH}_2)_6^*$  clusters frozen in their self-exchange partner geometries can be found in Table 2.

Values of  $\lambda_{\text{is}1}$  and  $\lambda_{\text{is}2}$  should be similar for self-exchange couples where the curvatures of the potential energy surfaces for the reactants are similar.<sup>26</sup> Calculated values of  $\lambda_{\text{is}1}$  and  $\lambda_{\text{is}2}$  are comparable within each set from this study, with exceptions for Cr and Co using DZVP and V using 6-311+G. The disagreement in these cases does not indicate a problem with

**TABLE 1: Calculated Inner Sphere Reorganization Energies for Self-Exchange (eV)<sup>a</sup>**

	Fe <sup>2+/3+</sup>	Cr <sup>2+/3+</sup>	Mn <sup>2+/3+</sup>	V <sup>2+/3+</sup>	Co <sup>2+/3+</sup>
B3LYP/DZVP					
$\lambda_{is1}$	0.331	0.863	0.984	0.535	0.165
$\lambda_{is2}$	0.349	0.416	1.030	0.498	0.436
$\lambda_{is}$	0.680	1.279	2.013	1.033	0.601
B3LYP/6-311+G					
$\lambda_{is1}$	0.320	1.025	0.884	0.499	0.291
$\lambda_{is2}$	0.291	0.905	0.904	0.363	0.394
$\lambda_{is}$	0.611	1.930	1.788	0.862	0.685
previous $\lambda_{is}$ calculs					
Delahay <sup>52</sup>	0.92	1.16	1.48	0.82	0.82
Bu et al. <sup>25</sup>	0.88	0.96	1.17	0.92	1.09
accepting orbital	$t_{2g}$	$e_g^*$	$e_g^*$	$t_{2g}$	$t_{2g}$

<sup>a</sup> The largest  $\lambda_{is}$  values are expected to correspond to the Cr(OH<sub>2</sub>)<sub>6</sub><sup>3+/2+</sup> self-exchange couple because it has the slowest observed rate and therefore the largest activation energy barrier. Mn and Cr self-exchanges both involve electron transfer into the antibonding  $e_g^*$  set of d-orbitals. This has a tendency to destabilize the complex and leads to relatively large changes in the configuration of the inner sphere H<sub>2</sub>O molecules and higher values of  $\lambda_{is}$ .

the approach, because the ab initio calculations account for anharmonicities in the potential energy surface, but the fact that it occurs for different M(OH<sub>2</sub>)<sub>6</sub> complexes depending on the basis set is an early demonstration of the basis set dependence inherent in this method.

In the final values of  $\lambda_{is}$ , however, both basis sets led to similar trends where Cr and Mn show higher inner sphere reorganization energies than Fe, V, and Co. This result is consistent with expectations from molecular orbital theory.  $\lambda_{is}$  can generally be correlated with the type of electron-accepting d-orbital on the metal atom. The reduction of both Cr(III) and Mn(III) involves the transfer of an electron into the  $e_g^*$  orbitals, which are the antibonding counterparts to the  $d_{z^2}$  and  $d_{x^2-y^2}$  bonding orbitals pointing toward the ligands. Occupation of the  $e_g^*$  d-orbitals causes substantial bond lengthening and distortion in the complex, leading to large inner sphere reorganization energies. In contrast, Fe(III) and V(III) accept the electron into nonbonding  $t_{2g}$  orbitals pointing between the ligands, equating to smaller changes in M–O bond length and lower  $\lambda_{is}$  energies. Likewise, because we have chosen to model the Co(II)/(III) self-exchange as a simple, high spin exchange, our calculations result in  $\lambda_{is}$  for Co that is similar in magnitude to that for Fe and V because high spin Co(III) accepts an electron into a  $t_{2g}$  nonbonding orbital.

Both basis sets also led to similar  $\lambda_{is}$  values for each particular M(OH<sub>2</sub>)<sub>6</sub> cluster, with the exception of Cr where the DZVP  $\lambda_{is}$  value is 0.65 eV below the 6-311+G value. We deem this exception as a failing in the series of calculations using the DZVP basis set. The observed Cr(II)/Cr(III) self-exchange rate is known to be the slowest of the five M(OH<sub>2</sub>)<sub>6</sub> complexes, and this can only be attributed to the largest  $\lambda_{is}$  energy for Cr of the five self-exchange couples, which was not the calculated result using DZVP.

Previous estimates of  $\lambda_{is}$  for comparison with our results are few and varied. Table 1 lists the theoretical estimates of  $\lambda_{is}$  by Delahay<sup>54</sup> and Bu et al.<sup>24</sup> The former takes the classical approach to calculating  $\lambda_{is}$  using a bond stretching model.<sup>55</sup> Bu et al. used a lower level of ab initio theory (restricted open shell Hartree–Fock/Slater-type orbital basis) to derive potential energy surfaces for the parametrization of electrostatic potentials. The parametrized force fields were used to calculate inner sphere reorganization energies for the M(OH<sub>2</sub>)<sub>6</sub> clusters. This approach was unable to take into account the large energy contributions from Jahn–Teller distortions in certain complexes, as opposed to the

**TABLE 2: Calculated Total Energies, Average Bond Lengths, and Symmetric Stretching Frequencies for the M(OH<sub>2</sub>)<sub>6</sub> Clusters in This Study<sup>a</sup>**

	Fe(II)(OH <sub>2</sub> ) <sub>6</sub>	Fe(III)(OH <sub>2</sub> ) <sub>6</sub>	Cr(II)(OH <sub>2</sub> ) <sub>6</sub>	Cr(III)(OH <sub>2</sub> ) <sub>6</sub>	Mn(II)(OH <sub>2</sub> ) <sub>6</sub>	Mn(III)(OH <sub>2</sub> ) <sub>6</sub>	V(II)(OH <sub>2</sub> ) <sub>6</sub>	V(III)(OH <sub>2</sub> ) <sub>6</sub>	Co(II)(OH <sub>2</sub> ) <sub>6</sub>	Co(III)(OH <sub>2</sub> ) <sub>6</sub>
B3LYP/DZVP										
$E_e$	-1721.7126	-1721.0659	-1502.5346	-1501.9379	-1609.0603	-1608.3950	-1402.1127	-1401.5194	-1840.7319	-1840.0383
G	-1721.6106	-1720.9557	-1502.4317	-1501.8289	-1608.9586	-1608.2871	-1402.0072	-1401.4066	-1840.6287	-1839.9289
av M–O bond length (Å)	2.050	2.154	2.063	2.190	2.031	2.201	2.040	2.160	2.036	2.121
sym stretch (cm <sup>-1</sup> )	397	329	434	347	442	315	437	339	383	337
$E_e^b$	-1721.6998	-1721.0537	-1502.5193	-1501.9061	-1609.0225	-1608.3588	-1402.0944	-1401.4997	-1840.7159	-1840.0323
B3LYP/6-311+G										
$E_e$	-1721.9030	-1721.3028	-1502.6779	-1502.1263	-1609.2258	-1608.5960	-1402.2388	-1401.6744	-1840.9433	-1840.2883
G	-1721.7953	-1721.1865	-1502.5714	-1502.0064	-1609.1190	-1608.4801	-1402.1278	-1401.5565	-1840.8330	-1840.1733
av M–O bond length (Å)	2.051	2.145	2.015	2.187	2.039	2.197	2.054	2.158	2.024	2.110
sym stretch (cm <sup>-1</sup> )	425	343	448	352	450	326	433	342	430	352
$E_e^b$	-1721.89229	-1721.29103	-1502.64469	-1502.088619	-1609.192516	-1608.563486	-1402.225508	-1401.6560	-1840.928837	-1840.27764

<sup>a</sup>  $E_e$  is the electronic energy (hartrees). G is the calculated free energy after accounting for the thermochemical contributions to the total energy for a 298.15 K, 1 atm standard state (zero point, thermal, enthalpic, and entropic corrections to the electronic energy). <sup>b</sup> A single point energy calculation was performed on the cluster in the frozen atomic configuration of the corresponding self-exchange partner.

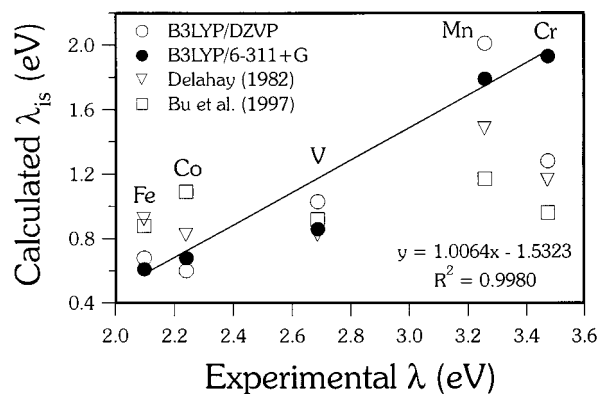


**Figure 3.** Comparison of various calculated inner sphere reorganization energies with the estimate of the experimental total reorganization energies for self-exchange reactions. For the series of  $M(\text{OH}_2)_6^{3+/2+}$  exchange reactions, the total reorganization energy is expected to be primarily due to reorganizing of the inner sphere  $\text{H}_2\text{O}$  molecules. Only the values calculated using the 6-311+G basis set lead to a good correlation (slope near 1), as can be seen by the linear regression for this data set (excludes V). The y-intercept is a rough estimate of the missing outer sphere contribution.

method used here. The differences between the values for  $\lambda_{\text{is}}$  from the various approaches in Table 1 are significant and would lead to large discrepancies in calculated rates.

The success of any of these methods must ultimately be judged based on a comparison with experiment. Since  $\lambda_{\text{is}}$  should correlate linearly, with a slope close to 1, with  $\lambda$  for this series, estimates of  $\lambda$  from experiment were obtained by applying the Marcus relations to experimental self-exchange rate data (see Theoretical Methods). Plots of our calculated  $\lambda_{\text{is}}$  vs the “best” estimate of  $\lambda$  from experimental rates (using  $x = 0 \text{ \AA}$ ) show that calculated  $\lambda_{\text{is}}$  from the previous studies and by use of DZVP in this study do not correlate well with  $\lambda$  from experiment (Figure 3). In contrast,  $\lambda_{\text{is}}$  calculated using the 6-311+G set shows a remarkably good slope  $\sim 1$  trend. The largest deviation in  $\lambda_{\text{is}}$  in this trend is due to  $\text{V}(\text{OH}_2)_6^{3+/2+}$ , which apparently is underestimated using B3LYP/6-311+G. Contradicting this conclusion is the fact that the various methods are in best agreement on  $\lambda_{\text{is}}$  values for this complex. This discrepancy remains unresolved. Excluding the V datum from the regression had little effect on the slope of the trend and reveals the remarkable correlation for the remaining four points (Figure 3), leading to the conclusion that the 6-311+G basis set significantly outperformed DZVP in the calculation of  $\lambda_{\text{is}}$ .

Using the 6-311+G basis set results, theoretical  $\lambda_{\text{os}}$  values were calculated using calculated values of  $r_{\text{M-O}}$  in eq 8 with the effective distance adjustment parameter  $x = 0$ . Summing  $\lambda_{\text{is}}$  and  $\lambda_{\text{os}}$ , we plotted our calculated  $\lambda$  against the best estimate of  $\lambda$  from experiment, linearly regressed all but the V datum, and then adjusted  $x$  to zero the intercept (Figure 4). The optimal value of  $x$  turned out to be  $0.56 \text{ \AA}$ . The slope of the linear trend in this plot can be seen to differ very little from that in Figure 3 because the differences in  $\lambda_{\text{os}}$  between the complexes are small; thus the slope is insensitive to  $R$ . This adjustment of  $x = 0.56 \text{ \AA}$  has the additional effect of improving the slope of the trend (closer to 1) because, although adjusting  $x$  primarily adjusted the theoretical value of  $\lambda_{\text{os}}$ , it also slightly adjusted the work correction applied to the experimental rate. The final values of the effective electron transfer distances and the corresponding work correction to  $k_{\text{obs}}$  for self-exchange are reported in Table 3, along with the best estimate for  $\lambda$  from the experimental rate data.

We used our calculated values of  $\lambda$ ,  $R$ ,  $\nu$ , and  $\kappa$  to predict the observed rates of exchange at the ionic strengths used in the

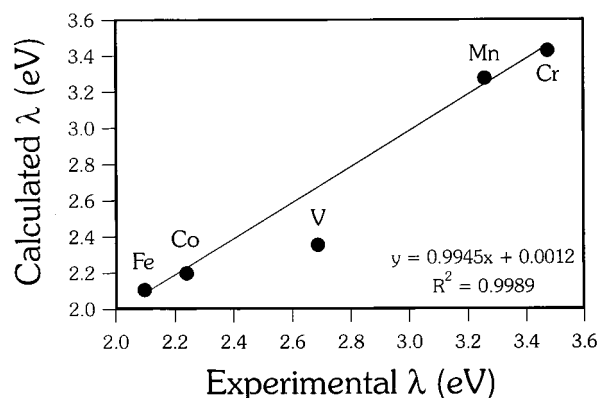


**Figure 4.** Calculated total reorganization energies for self-exchange using the 6-311+G set with the adjustable effective electron transfer distance parameter  $x = 0.56 \text{ \AA}$ . This value was determined by adjusting  $x$  to zero the y-intercept in the trend (excluding V). This also had the possibly fortuitous effect of improving the slope of the trend by bringing it closer to a value of 1.

experiments. Calculated values for  $\kappa$  [ $0.060$  ( $\text{Fe}(\text{OH}_2)_6^{3+/2+}$ ),  $0.098$  ( $\text{Cr}(\text{OH}_2)_6^{3+/2+}$ ),  $0.068$  ( $\text{Mn}(\text{OH}_2)_6^{3+/2+}$ ),  $0.013$  ( $\text{V}(\text{OH}_2)_6^{3+/2+}$ ),  $0.042$  ( $\text{Co}(\text{OH}_2)_6^{3+/2+}$ )] are in reasonable agreement with those calculated elsewhere.<sup>53</sup> The resulting rates are reported in Table 4, where the agreement can easily be seen to be satisfactory when one considers that an entirely outer sphere pathway is assumed and approximate expressions for  $\lambda_{\text{os}}$  are being utilized. However, as can be predicted from Figure 3, the calculated  $\text{V}(\text{OH}_2)_6^{3+/2+}$  self-exchange rate is somewhat higher than the observed rate. A variety of possible reasons could lead to this result, including a failing in the B3LYP/6-311+G description of one or more of the  $\text{V}(\text{OH}_2)_6$  complexes, and/or inapplicability of the above assumptions to the  $\text{V}(\text{OH}_2)_6^{3+/2+}$  self-exchange. Regarding the latter, evidence has been presented indicating that many V(II) reactions proceed by a bridged mechanism,<sup>28</sup> but this would have the tendency to result in faster observed rates than the predicted outer sphere rates.

Very little information is available in the literature where the value of  $R$  has been addressed in detail from a standpoint independent of inference via the Marcus treatment. Values in the range  $7\text{--}8 \text{ \AA}$  have most commonly been used in earlier treatments of  $M(\text{OH}_2)_6$  complexes.<sup>29,56</sup> However, there is contrasting evidence in a study of a variety of Ru complexes of different sizes, suggesting that  $R$  is best approximated by a simple sum of the “hard-sphere” reactant radii.<sup>57</sup> The estimates for  $R$  in this study fall in a narrow range of  $5.2\text{--}5.4 \text{ \AA}$ . Furthermore, a previous theoretical investigation of the Fe(II)/Fe(III) exchange indicates  $R = 5.25 \text{ \AA}$  for this couple,<sup>58</sup> much smaller than the traditional values of  $7\text{--}8 \text{ \AA}$ . For the Fe(II)/Fe(III) exchange couple, we arrive at a small value for  $R$  ( $5.3 \text{ \AA}$ ) that agrees surprisingly well with Tembe and co-workers<sup>58</sup> and is closer to the sum of reactant radii than traditional values.

**Bimolecular Redox Reactions.** The Marcus equations are easily extended from self-exchange to bimolecular redox reactions in solution, assuming an outer sphere pathway, with knowledge of the free energy change from the precursor to successor state for the reaction ( $\Delta G^\circ$ ). This energy, typically derived from formal reduction potentials, can also be estimated from ab initio total energy calculations, leading to the ability to predict cross reaction rates entirely from theory using the methods described here. An in-depth investigation of the mechanisms of cross reactions involving the  $M(\text{OH}_2)_6$  complexes is beyond the scope of this study, and because our calculated intrinsic exchange barriers are consistent with experiment, little new information would be gained with the current

**TABLE 3: Best Estimates for the Total Reorganization Energy and Related Parameters from Experimental Rates Compared to Calculated Total Reorganization Energies<sup>a</sup>**

	Fe <sup>2+/3+</sup>	Cr <sup>2+/3+</sup>	Mn <sup>2+/3+</sup>	V <sup>2+/3+</sup>	Co <sup>2+/3+</sup>
B3LYP/6-311+G					
<i>R</i> (Å)	5.32	5.32	5.36	5.33	5.25
<i>ν</i> (s <sup>-1</sup> )	1.16 × 10 <sup>13</sup>	1.21 × 10 <sup>13</sup>	1.18 × 10 <sup>13</sup>	1.17 × 10 <sup>13</sup>	1.18 × 10 <sup>13</sup>
<i>κ</i>	0.060	0.098	0.068	0.013	0.042
<i>λ</i> <sub>is</sub> (eV)	0.611	1.930	1.788	0.862	0.685
<i>λ</i> <sub>os</sub> (eV)	1.502	1.521	1.509	1.494	1.524
<i>λ</i> (eV)	2.11	3.45	3.30	2.36	2.21
experimental					
<i>k</i> <sub>obs</sub> (M <sup>-1</sup> s <sup>-1</sup> )	4.2 (0.6)	2.0 × 10 <sup>-5</sup> (1)	3.0 × 10 <sup>-4</sup> (3)	1.0 × 10 <sup>-2</sup> (2)	3.3 (3)
<i>w</i> (J/mol)	8720.0	7276.5	4910.3	5740.8	5078.1
<i>K</i> <sub>pre</sub> (M <sup>-1</sup> )	0.178	0.179	0.181	0.179	0.174
<i>k</i> <sub>et</sub> (s <sup>-1</sup> )	7.9 × 10 <sup>2</sup>	2.1 × 10 <sup>-3</sup>	1.2 × 10 <sup>-2</sup>	5.7 × 10 <sup>-1</sup>	1.5 × 10 <sup>2</sup>
<i>ΔG</i> <sup>*</sup> (J/mol)	51345.7	85851.2	79567.4	69674.7	55594.0
<i>λ</i> (eV)	2.10	3.47	3.26	2.69	2.24

<sup>a</sup> The calculated values for *R*, including *x* = 0.56 Å, were used both to treat the experimental rate data using Marcus theory and to calculate *λ*<sub>os</sub>. Calculated values for *ν* and *κ* were also used in treating the experimental data. Observed rates were taken from ref 29. The experimental ionic strengths are listed in parentheses.

**TABLE 4: Comparison of Observed Self-Exchange Rates with Those Calculated for Similar Ionic Strength Conditions (*μ*), Using B3LYP/6-311+G**

	Fe <sup>2+/3+</sup> <i>μ</i> = 0.6	Cr <sup>2+/3+</sup> <i>μ</i> = 1.0	Mn <sup>2+/3+</sup> <i>μ</i> = 3.0	V <sup>2+/3+</sup> <i>μ</i> = 2.0	Co <sup>2+/3+</sup> <i>μ</i> = 3.0
<i>k</i> <sub>obs</sub>	4.2	2.0 × 10 <sup>-5</sup>	3.0 × 10 <sup>-4</sup>	1.0 × 10 <sup>-2</sup>	3.3
<i>k</i> <sub>calcd</sub>	4.9	3.7 × 10 <sup>-5</sup>	2.8 × 10 <sup>-4</sup>	3.0 × 10 <sup>-1</sup>	5.6
log <i>k</i> <sub>obs</sub>	0.6	-4.7	-3.5	-2.0	0.5
log <i>k</i> <sub>calcd</sub>	0.7	-4.4	-3.6	-0.5	0.7

**TABLE 5: Comparison of Calculated and Experimental *ΔG*<sup>o</sup> for Bimolecular Electron Transfer Reactions (kJ/mol)<sup>a</sup>**

	B3LYP/DZVP	B3LYP/6-311+G	expt
Fe(III) <sub>aq</sub> + Cr(II) <sub>aq</sub> →	-137.072	-115.123	-113.677
Fe(II) <sub>aq</sub> + Cr(III) <sub>aq</sub> →			
Fe(II) <sub>aq</sub> + Mn(III) <sub>aq</sub> →	-43.544	-79.046	-74.353
Fe(III) <sub>aq</sub> + Mn(II) <sub>aq</sub> →			

<sup>a</sup> Experimental values are derived from formal reduction potentials. Calculated values are the calculated free energy changes after accounting for the thermochemical contributions to the total energy for a 298.15 K, 1 atm standard state (zero point, thermal, enthalpic, and entropic corrections to the electronic energy).

treatment. However, it is prudent to evaluate the accuracy of calculated *ΔG*<sup>o</sup> using DFT methods to complete the description of the usefulness of the ab initio approaches to predict outer sphere electron transfer rates. Only a few such cross reactions are thought to follow an outer sphere pathway<sup>28</sup> where the Marcus treatment is appropriately applied in some form, so we accordingly chose Fe(III)/Cr(II)<sup>59</sup> and Fe(II)/Mn(III).<sup>60,61</sup>

A comparison of experimental vs calculated *ΔG*<sup>o</sup> for the two bimolecular reactions is given in Table 5, including thermochemical corrections to the electronic energy. It should be noted that Gaussian94 uses a 298.15 K, 1 atm ideal gas standard state which leads to an underestimation in the total free energy of the molecule in solution by approximately 8 kJ/mol.<sup>45</sup> This error is canceled out in the calculation of *ΔG*<sup>o</sup>, however. In Table 5, it can be seen that the 6-311+G basis set leads to relatively accurate estimations of *ΔG*<sup>o</sup> for these reactions, agreeing with experiment values within about 4 kJ/mol, which are more than satisfactory for application within the Marcus relations. In contrast, the DZVP set leads to *ΔG*<sup>o</sup> estimations that are 24–31 kJ/mol off and can be considered no better than about 70% accurate on average for these reactions. Both basis sets lead to ~29 kJ/mol (6-311+G) and 16–59 kJ/mol (DZVP) underestimations of *ΔG*<sup>o</sup> for cross reactions involving Co, presumably due to our high spin assumption for Co(III).

**TABLE 6: Comparison of Observed Bimolecular Electron Transfer Rates<sup>59,61</sup> with Those Calculated for Similar Ionic Strength Conditions (*μ*)**

	Fe(III) + Cr(II) → Fe(II) + Cr(III)	Fe(II) + Mn(III) → Fe(III) + Mn(II)
experiment		
<i>μ</i> (M)	1	3
<i>k</i> <sub>obs</sub> (M <sup>-1</sup> s <sup>-1</sup> )	2.30 × 10 <sup>3</sup>	1.02 × 10 <sup>4</sup>
B3LYP/6-311+G		
<i>ΔG</i> <sup>o</sup> (kJ/mol)	-115.12	-79.05
<i>λ</i> (kJ/mol)	293.51	286.00
<i>ΔG</i> <sup>*</sup> (kJ/mol)	27.10	37.44
<i>ν</i> (s <sup>-1</sup> )	1.18 × 10 <sup>13</sup>	1.17 × 10 <sup>13</sup>
<i>κ</i>	0.076	0.063
<i>k</i> <sub>et</sub> (s <sup>-1</sup> )	1.46 × 10 <sup>8</sup>	2.28 × 10 <sup>6</sup>
<i>R</i> (Å)	5.36	5.31
<i>w</i> (kJ/mol)	7196.5	4968.7
<i>K</i> <sub>pre</sub> (M <sup>-1</sup> )	9.93 × 10 <sup>-3</sup>	2.39 × 10 <sup>-2</sup>
<i>k</i> (M <sup>-1</sup> s <sup>-1</sup> )	1.45 × 10 <sup>6</sup>	5.44 × 10 <sup>4</sup>

In Table 6, we compare observed rates for the two redox reactions vs those predicted for the corresponding experimental ionic strengths using the 6-311+G basis set calculations. The calculated overall rate of the Fe(III) + Cr(II) reaction is about 3 orders of magnitude too fast. Similar overestimations have been the result in previous predictive studies.<sup>56</sup> In contrast, the calculated rate for the Fe(II) + Mn(III) reaction agrees remarkably well with experiment. The Fe(III) + Cr(II) reaction involves the transfer of an electron from a t<sub>2g</sub> orbital to an e<sub>g</sub>\* orbital, and the Fe(II) + Mn(III) reaction involves the transfer of an electron from an e<sub>g</sub>\* orbital to a t<sub>2g</sub> orbital. Since, from molecular orbital theory, the direct electron transfer for both processes are symmetry inhibited, the reactants presumably should have similar propensities to react. Likewise, ligand exchange rates of at least one of the reactants in each equation are slower than the overall redox reactions;<sup>52</sup> therefore the tendencies toward an outer sphere pathway should be roughly similar. There are a variety of neglected factors that could lead to the overestimation of the Fe(II) + Cr(III) rate, many of which have been inconclusively scrutinized elsewhere in the literature.<sup>56</sup> Nevertheless, the B3LYP/6-311+G calculations applied here to lead to predictions of *ΔG*<sup>o</sup> that are sufficiently accurate to be useful in the Marcus treatment of these bimolecular redox reactions.

## 5. Conclusions

Inner sphere reorganization energies calculated using the ab initio approach of Klimkans and Larsson lead to useful and

accurate values, assuming care is taken with choice of basis set and ab initio method. The variability in the observed self-exchange rates for  $M(OH_2)_6$  complexes is predominantly due to the energy to reorganize the first hydration sphere. Jahn–Teller contributions are conveniently and accurately included in the calculated  $\lambda_{is}$  value. This theoretical approach is, to our knowledge, the first to lead to  $\lambda_{is}$  values that properly correlate with observed self-exchange rates for the hexaquo ions in this study. The effective electron transfer radii of these metal ions are estimated to be slightly larger than the average M–O bond distance, in agreement with conclusions elsewhere that  $R$  is closely approximated by hard-sphere radii of the reactants. Relative B3LYP/6-311+G total energies for all but Co hexaquo ions in this study provide excellent estimates of the driving force for the electron transfer step.

The methods discussed here provide a convenient means to produce reasonably accurate estimates of the Marcus parameters  $\lambda$ ,  $\nu$ ,  $\kappa$ ,  $R$ , and  $\Delta G^\circ$  to estimate outer sphere electron transfer rates. Marcus' theory provides the unique ability to predict observable rates at the macroscopic scale using only molecular scale information on the elementary electron transfer step. In a broader perspective, the methods employed here could easily be extended to a wide variety of reactants where necessary experimental data are unavailable and/or difficult to acquire. Such systems include outer sphere electron transfer as a function of speciation, and also heterogeneous electron transfer at interfaces, the subject of future work.

**Acknowledgment.** The authors thank Andy Felmy for helpful discussions during the course of this study. Jodi Rosso made significant scientific and editorial improvements to the manuscript. This research was supported by the Office of Basic Energy Science (BES), Geosciences Program, U.S. Department of Energy (DOE). Pacific Northwest National Laboratory is operated for the DOE by Battelle Memorial Institute under Contract No. DE-AC06-76RLO 1830.

## References and Notes

- (1) Diem, D.; Stumm, W. *Geochim. Cosmochim. Acta* **1984**, *48*, 1571.
- (2) Chen, K. Y.; Morris, C. J. *Environ. Sci. Technol.* **1972**, *6*, 529.
- (3) Luther, G. W., III. The frontier-molecular orbital theory approach in geochemical processes. In *Aquatic Chemical Kinetics*; Stumm, W., Ed.; John Wiley & Sons: New York City, 1990; p 173.
- (4) Stone, A. T. Adsorption of organic reductants and subsequent electron transfer on metal oxide surfaces. In *Geochemical Processes at Mineral Surfaces*; Davis, J. A., Hayes, K. F., Eds.; American Chemical Society: Washington, DC, 1986; Vol. 323, p 446.
- (5) Voudrias, E. A.; Reinhard, M. Abiotic organic reactions at mineral surfaces. In *Geochemical Processes at Mineral Surfaces*; Davis, J. A., Hayes, K. F., Eds.; American Chemical Society: Washington, DC, 1986; Vol. 323, p 462.
- (6) Van Cappellen, P.; Gaillard, J.-P. Biogeochemical dynamics in aquatic systems. In *Reactive transport in porous media*; Lichtner, P. C., Oelkers, E. H., Eds.; Mineralogical Society of America: Washington, DC, 1996; Vol. 34, p 335.
- (7) Steefel, C. I.; MacQuarrie, K. T. B. Approaches to modeling of reactive transport in porous media. In *Reactive transport in porous media*; Lichtner, P. C., Oelkers, E. H., Eds.; Mineralogical Society of America: Washington, DC, 1996; Vol. 34, p 83.
- (8) McNab, W. W.; Narasimhan, T. N. *Water Resour. Res.* **1994**, *30*, 2610.
- (9) Keating, E. H.; Bahr, J. M. *Water Resour. Res.* **1998**, *34*, 3573.
- (10) Nordin, J. P.; Sullivan, D. J.; Phillips, B. L.; Casey, W. H. *Inorg. Chem.* **1998**, *37*, 4760.
- (11) Marcus, R. A. *J. Chem. Phys.* **1956**, *24*, 966.
- (12) Marcus, R. A. *J. Phys. Chem.* **1990**, *94*, 1050.
- (13) Marcus, R. A.; Sutin, N. *Biochim. Biophys. Acta* **1985**, *811*, 265.
- (14) Eggleston, C. M.; Ehrhardt, J. J.; Stumm, W. *Am. Mineral.* **1996**, *81*, 1036.
- (15) Eggleston, C. M. *Am. Mineral.* **1999**, *84*, 1061.
- (16) Tao, N. J. *Phys. Rev. Lett.* **1996**, *76*, 4066.
- (17) Muller, R. P.; Warshel, A. J. *Phys. Chem.* **1995**, *99*, 17516.
- (18) Straus, J. B.; Calhoun, A.; Voth, G. A. *J. Chem. Phys.* **1995**, *102*, 529.
- (19) Smith, B. B.; Nozik, A. J. *J. Phys. Chem. B* **1997**, *101*, 2459.
- (20) German, E. D.; Kuznetsov, A. M. *J. Phys. Chem. A* **1998**, *102*, 3668.
- (21) Ando, K. *J. Chem. Phys.* **1997**, *106*, 116.
- (22) Bader, J. S.; Cortis, C. M.; Berne, B. J. *J. Chem. Phys.* **1997**, *106*, 2372.
- (23) Bu, Y.; Song, X. *J. Phys. Chem.* **1994**, *98*, 5049.
- (24) Bu, Y. X.; Ding, Y. J.; He, F. X.; Jiang, L. F.; Song, X. Y. *Int. J. Quantum Chem.* **1997**, *61*, 117.
- (25) Bu, Y. X.; Wang, Y. X.; Xu, F. Q.; Deng, C. H. *J. Mol. Struct.* **1998**, *453*, 43.
- (26) Klimkans, A.; Larsson, S. *Chem. Phys.* **1994**, *189*, 25.
- (27) Jakobsen, S.; Mikkelsen, K. V.; Pedersen, S. U. *J. Phys. Chem.* **1996**, *100*, 7411.
- (28) Rosseinsky, D. R. *Chem. Rev.* **1972**, *72*, 215.
- (29) Sutin, N. Theory of electron transfer reactions. In *Electron transfer and electrochemical reactions; Photochemical and other energized reactions*; Zuckermann, J. J., Ed.; VCH: New York, 1986; Vol. 15, p 16.
- (30) Siefert, R. L.; Johansen, A. M.; Hoffmann, M. R.; Pehkonen, S. O. *J. Air Waste Manage. Assoc.* **1998**, *48*, 128.
- (31) Creutz, C.; Sutin, N. General reactivity patterns in electron transfer. In *Electron transfer and electrochemical reactions; Photochemical and other energized reactions*; Zuckermann, J. J., Ed.; VCH: New York, 1986; Vol. 15; p 16.
- (32) Gratzel, M. *Heterogeneous photochemical electron transfer*; CRC Press: Boca Raton, FL, 1989.
- (33) Wehrli, B. Redox reactions of metal ions at mineral surfaces. In *Aquatic Chemical Kinetics*; Stumm, W., Ed.; John Wiley & Sons: New York City, 1990; p 311.
- (34) Miller, J. R. *Nuov. J. Chim.* **1987**, *11*, 82.
- (35) Weaver, M. J.; Lee, E. L. *Inorg. Chem.* **1980**, *19*, 193.
- (36) Robinson, R. A.; Stokes, R. H. *Electrolyte solutions*; Butterworth Scientific Publications: London, 1955.
- (37) Garrels, R. M.; Christ, C. L. *Solutions, Minerals, and Equilibria*; Harper, Row & Brothers: New York, 1965.
- (38) Newton, M. D. *J. Phys. Chem.* **1986**, *90*, 3734.
- (39) Newton, M. D. *J. Phys. Chem.* **1988**, *92*, 3049.
- (40) Marcus, R. A. *J. Chem. Phys.* **1957**, *26*, 867.
- (41) Frisch, M. J.; Trucks, G. W.; Schlegel, H. B.; Gill, P. M. W.; Johnson, B. G.; Robb, M. A.; Cheeseman, J. R.; Keith, T. A.; Petersson, G. A.; Montgomery, J. A.; Raghavachari, K.; Al-Laham, M. A.; Zakrzewski, V. G.; Ortiz, J. V.; Foresman, J. B.; Cioslowski, J.; Stefanov, B. B.; Nanayakkara, A.; Challacombe, M.; Peng, C. Y.; Ayala, P. Y.; Chen, W.; Wong, M. W.; Andres, J. L.; Replogle, E. S.; Gomperts, R.; Martin, R. L.; Fox, D. J.; Binkley, S.; Defrees, D. J.; Baker, J.; Stewart, J. J. P.; Head-Gordon, M.; Gonzalez, C.; Pople, J. A. *Gaussian94*, Revision C.2; Gaussian, Inc.: Pittsburgh, PA, 1995.
- (42) Becke, A. D. *J. Chem. Phys.* **1993**, *98*, 1372.
- (43) Lee, C.; Yang, W.; Parr, R. G. *Phys. Rev. B* **1988**, *37*, 785.
- (44) Ricca, A.; Bauschlicher, C. W. *J. Phys. Chem.* **1994**, *98*, 12899.
- (45) Russo, T. V.; Martin, R. L.; Hay, P. J. *J. Phys. Chem.* **1995**, *102*, 8023.
- (46) Martin, R. L.; Hay, P. J.; Pratt, L. R. *J. Phys. Chem. A* **1998**, *102*, 3565.
- (47) Rustad, J. R.; Dixon, D. A.; Rosso, K. M.; Felmy, A. R. *J. Am. Chem. Soc.* **1999**, *121*, 3234.
- (48) Godbout, N.; Salahub, D. R.; Andzelm, J.; Wimmer, E. *Can. J. Chem. Rev. Can. Chim.* **1992**, *70*, 560.
- (49) Wachters, A. J. H. *J. Chem. Phys.* **1970**, *52*, 1033.
- (50) Hay, P. J. *J. Chem. Phys.* **1977**, *66*, 4377.
- (51) Clark, T.; Chandrasekhar, J.; Spitznagel, G. W.; Shleyer, P. v. R. *J. Comput. Chem.* **1983**, *4*, 294.
- (52) Richens, D. T. *The chemistry of aqua ions*; Wiley: New York, 1997.
- (53) Bu, Y. X.; Deng, C. H. *J. Phys. Chem. A* **1997**, *101*, 1198.
- (54) Delahay, P. *Chem. Phys. Lett.* **1982**, *87*, 607.
- (55) Marcus, R. A. *J. Phys. Chem.* **1963**, *67*, 853.
- (56) Hupp, J. T.; Weaver, M. J. *Phys. Chem.* **1985**, *89*, 2795.
- (57) Brown, G. M.; Sutin, N. *J. Am. Chem. Soc.* **1979**, *101*, 883.
- (58) Tembe, B. L.; Friedman, H. L.; Newton, M. D. *J. Phys. Chem.* **1982**, *76*, 1490.
- (59) Dulz, G.; Sutin, N. *J. Am. Chem. Soc.* **1964**, *86*, 829.
- (60) Diebler, H.; Sutin, N. *J. Phys. Chem.* **1964**, *68*, 174.
- (61) Rosseinsky, D. R.; Nicol, M. J. *Trans. Faraday Soc.* **1968**, *64*, 2410.